Appl. Phys. B 80, 351–354 (2005)
DOI: 10.1007/s00340-005-1729-1

Applied Physics B
Lasers and Optics

L. ARIZMENDI[1, ✉]
V. DE ANDRÉS[1]
E.M. DE MIGUEL-SANZ[2]
M. CARRASCOSA[1]

Determination of proton diffusion anisotropy by thermal decay of fixed holograms with *K*-vector perpendicular to the *c*-axis in $LiNbO_3$:Fe

[1]Dept. Física de Materiales, C-IV, Universidad Autónoma de Madrid-28049 Madrid, Spain
[2]Dept. Óptica y Optometría, Universidad Europea de Madrid-28670 Villaviciosa de Odón, Spain

Received: 4 October 2004 /
Revised version: 25 November 2004
Published online: 4 February 2005 • **© Springer-Verlag 2005**

ABSTRACT In this paper the thermal fixing of holographic gratings with *K*-vectors perpendicular to the crystallographic *c*-axis of $LiNbO_3$ is considered in order to obtain information about anisotropy of the proton thermal diffusion in this crystal. Specifically, thermal decays of fixed holograms in particular crystallographic directions are measured and related with proton diffusion. The values obtained are compared with previous data of decays of fixed holograms with *K*-vector parallel to the *c*-axis. The results show a high anisotropy of the thermal diffusion of protons in lithium niobate crystals.

PACS 42.40 Lx; 42.70 Ln; 42.70 Nq

1 Introduction

Since the discovery of thermal fixing of photorefractive holograms in iron doped lithium niobate in 1971 by Amodei and Staebler [1], much work has been done in this field. The ionic charges responsible of this phenomenon were well identified as protons (H^+) bonded to the regular oxygen ions of the crystal [2–4]. The optimum temperatures of fixing were also profusely studied [5, 6]. There are two rather different procedures to fix a grating. The sequential thermal fixing procedure consists in the room temperature recording of the hologram followed by heating to a temperature in the range of 140–180°C. In this process the ionic charges form a replica of the recorded electronic grating by screening the internal electric fields. Finally, again at room temperature the electronic grating is partially reduced and shifted by means of uniform light illumination. The uncompensated ionic grating presents the same diffraction properties as the original hologram. An alternative procedure, the simultaneous fixing method, consists in recording the hologram at high temperature. Hence ion compensation proceeds simultaneously to recording. In comparison with the former fixing method the result in this case is a much deeper grating amplitude but with a slightly different period from that recorded at high temperature.

Studies of time stability of fixed holograms at different temperatures [4] allowed us to obtain interesting information on the photorefractive material. At constant temperatures in the range 60–120°C, single exponential time decays of the fixed hologram diffraction efficiency, under uniform illumination, are observed. The activation energy of proton diffusion was then obtained to be $E_a = 0.95$ eV. As predicted by the theory [7], the decay rates depended on the concentration of protons (hydrogen), on the relative concentrations of donors (Fe^{2+}) and acceptors (Fe^{3+}) in the sample, as well as on the grating spatial frequency K. The specific dependences on these parameters are given by

$$\Gamma = D_H K^2 [(H_0/N_T) + 1], \quad (1)$$

where Γ is the decay rate, H_0 the concentration of hydrogen, $N_T = N_A N_D/(N_A + N_D)$ is the effective trap concentration, N_A and N_D are the electron acceptor [Fe^{3+}] and donor [Fe^{2+}] concentration respectively, D_H the thermal diffusion coefficient of the protons. The dependence with the temperature comes from this latter coefficient, D_H, which follows an Arrhenius law:

$$D_H = D_{H0} \exp(-E_A/k_B T). \quad (2)$$

Here D_{H0} is the diffusion preexponential factor, k_B the Boltzman's constant and T the absolute temperature of the sample. Using samples with different hydrogen and effective trap concentrations this dependence was demonstrated experimentally [4] and the determined diffusion coefficient is included in Table 1. More details and comments on this determination can be found in Ref. [4].

In fact this coefficient corresponds to the diffusion of protons in the direction of the *c*-axis of the crystal. Note that the common $LiNbO_3$ sample orientation for holographic recording, which takes advantage of the highest photovoltaic and electrooptic tensor coefficients, is that with the *c*-axis lying on the incidence plane of recording beams. Then the grating *K*-vector is parallel to the *c*-axis, and so the charge distribution planes are perpendicular to this axis. In all photorefractive

✉ Fax: +34-91-4978579, E-mail: luis.arizmendi@uam.es

fixing measurements done so far, the holograms were oriented in that direction, i.e. with the grating K-vector oriented along the c-axis. In particular, this is so in our former measurements of fixed hologram decays [4], i.e. the H^+ ions had to shift along the c direction to result in the decay of the fixed holograms.

On the other hand, in lithium niobate the infrared OH^- stretching absorption band is absolutely σ-polarized [8], i.e. only the light with its electric field polarized in perpendicular to the crystal c-axis is absorbed by this center. Similar dichroism behavior has been observed in other non-cubic oxides such as TiO_2 [9], and Al_2O_3 [10]. In all cases this is attributed to the orientation of the O—H bond along a direction perpendicular to the c-axis. In the model for $LiNbO_3$ the proton is lying in the oxygen plane perpendicular to the c-axis and the bond is directed towards one of the six nearest O^{2-} ions. As the O—O distances are not equivalent, this gives rise to absorption sub-bands [11]. In view of this model, it is reasonable to expect that diffusion of protons, jumping from oxygen to oxygen, has different diffusion characteristics along the c-axis than along its perpendicular. Then, some anisotropy in the diffusion coefficient should be expected, as it is the case for TiO_2 crystals [9]. However, the macroscopic hydrogen diffusion measurements did not seem to detect such anisotropy [12]. The aim of this work is to use the photorefractive thermal fixing technique to clarify this point determining whether there is anisotropy of proton diffusion in lithium niobate crystals. In fact, thermal decay of photorefractive fixed gratings, because of the extension of the photorefractive gratings, deals with the diffusion of protons in the bulk material. In contrast, macroscopic hydrogen diffusion measurements usually obtain results about the faster movement of hydrogen likely along dislocations and other defects.

2 Experimental methods

The holographic gratings were recorded by using a conventional two wave mixing setup. The recording wavelength was 514.5 nm from a CW Ar^+ laser. Both beams were expanded to cover all the sample face in order to avoid spatial charge accumulation. In this experiment the beam crossing angle was fixed in a value of 58°, which leads to an interference pattern spacing of 0.53 μm. Two samples of $10 \times 10 \times 2$ mm in size, with their bigger faces perpendicular either to the x (x-cut sample) or y (y-cut sample) crystallographic axes respectively, were cut from congruent $LiNbO_3$:Fe monodomain crystals. The iron doping was 0.1% mol in the melt for both samples, but they differed in the $[Fe^{2+}/Fe^{3+}]$ ratio and in the OH^- concentration. The y-cut sample had $[Fe^{2+}/Fe^{3+}] = 4.4 \times 10^{-2}$ and $[OH^-] = 4.5 \times 10^{18}$ cm^{-3}, whereas the x-cut sample had $[Fe^{2+}/Fe^{3+}] = 2.1 \times 10^{-2}$ and $[OH^-] = 5.3 \times 10^{18}$ cm^{-3}, determined from the optical absorption spectra as described elsewhere [13, 14].

For the measurements included in this study the samples were oriented with their z-axis in perpendicular to the beam incidence plane. Then the grating vector is either parallel to the y or x axis depending on the particular sample considered. Fixing was produced by the sequential fixing method, heating the sample at 150°C during 15 min after recording. After fixing the sample was cooled down to a given lower temperature and illuminated with uniform white light from two 150 W halogen lamps for developing. This illumination was maintained on the sample during all the measuring time. One of the recording beams with its intensity limited to 10 mW/cm^2 was used as probe beam. We probed experimentally that this beam had no effect on the decay rates, as it was expected for the behaviour of a fixed hologram which is continuously developed by the white light. The intensities of the diffracted and transmitted parts of the probe beam were measured and the diffraction efficiency calculated using the expression $\eta = I_{\text{diff}}/(I_{\text{diff}} + I_{\text{trans}})$.

3 Experimental results and discussion

Each single measurement consisted in monitoring the diffracted efficiency during the time the grating is decaying at a given temperature. To our knowledge this is the first time that holograms with K-vectors oriented in perpendicular to the c-axis are fixed in lithium niobate. We expected diffraction efficiency lower than that observed in the usual orientation due to the fact that the main photovoltaic contribution in lithium niobate is along the c-axis. We obtained a diffraction efficiency a little higher than 10% for fixed holograms in the x-cut sample, whereas the highest diffraction efficiency for the y-cut sample was only a little less than 1%. Although the value of diffraction efficiency is not essential for our method of determining proton diffusion coefficient, let us briefly discuss the origin of these lower values.

In fact the high diffraction efficiency of regular holograms recorded in lithium niobate is due to two important factors, the bulk photovoltaic effect and the electrooptic effect. Both effects are of tensorial nature, and in both cases the highest tensor elements are those involved in the orientation with K-vector parallel to the z-axis [15, 16]. Notwithstanding, both tensors have nonvanishing elements acting for holograms with K-vector in the x and y directions. Specifically, for hologram recording in this work we used light polarization parallel to the z-axis. According to the tensorial properties of the photovoltaic effect in this material [17], there is almost no photovoltaic current in the direction of charge movement (the x or y direction depending on the case) during recording of our holograms. So electronic charge diffusion instead the bulk photovoltaic effect must be the main contribution to the charge transport during recording of these holograms. Once the charge grating is formed, the index change distribution is provided by the electrooptic effect. In our new hologram orientations the main electrooptic tensor element involved is r_{42} which value is relatively high in lithium niobate, $r_{42} = 32.6$ pm/V [15]. On the other hand, the photovoltaic effect plays also an important role in the developed diffraction efficiency of fixed holograms [14]. In contrast with the recording, and according with [17], there is an effective photovoltaic effect for developing in the x-cut sample, due to that we are using nonpolarized light for developing. For the y-cut sample this effect does not appear. All this explains the nonzero but relatively low diffraction efficiency and the differences in diffraction efficiency observed between the x-cut and y-cut samples.

In any case, for our decay measurements the initial diffraction efficiency was limited to less than 1%. Under this condition the diffraction efficiency can be considered proportional to the square of the refractive index change amplitude forming

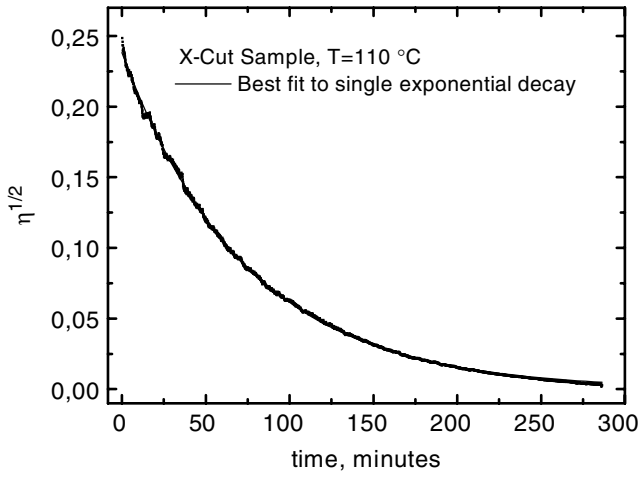

FIGURE 1 Plot of the time evolution of square root of the diffraction efficiency of a hologram fixed in a $LiNbO_3$:Fe x-cut sample. K-vector is oriented in the y direction. Sample temperature is 110°C. The line corresponds to the best fit of data points to a single exponential dependence

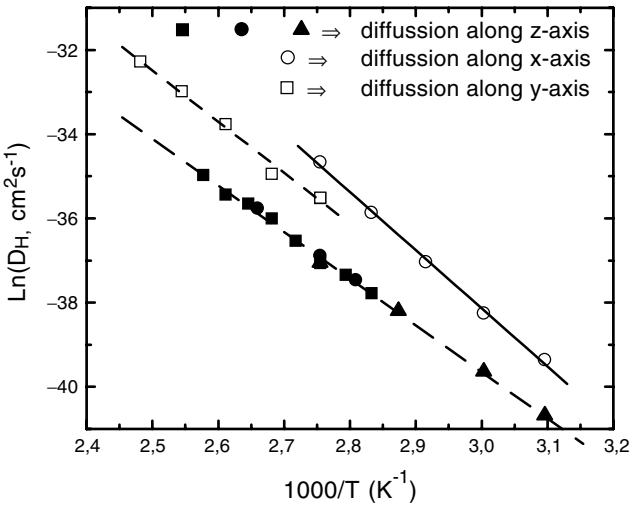

FIGURE 2 Plot of the logarithm of the proton diffusion coefficients determined from experimental hologram decay data by means of expression (1) for three different samples. Lines correspond to the best fits to straight lines

the holographic grating. Respectively, this index change is proportional to the space charge electric field amplitude. Thus, we are interested in the square root of the low valued diffraction efficiency.

In all our measurements the plot of square root of the diffraction efficiency against time could be well fitted to a single exponential with no background level. Figure 1 shows an example of decay plot and the corresponding fitting line (almost indistinguishable from the data points). The same dependence appeared also in our previous work for holographic gratings parallel to the c-axis. This fact means that the decay has to be attributed to a single process. We obtained the decay rate parameters for each sample at different temperatures. From the measured decay rates and using (1) we obtained the diffusion coefficients for each temperature and sample. The observed increase of the diffusion coefficient with temperature indicates that the involved process is thermally activated. In order to compare with theory we plotted in Fig. 2 the logarithm of the diffusion coefficient versus the inverse absolute temperature. For each sample the points appear ordered in a straight line, as predicted by Eq. 2. This means that a well defined activation energy exists for the temperature dependence of hydrogen diffusion in each sample.

Values of the preexponential factors and activation energies resulted from fittings are presented in Table 1, together with the values obtained for z-axis diffusion in our former paper [4]. The obtained activation energies, as well as the preexponential factor, account for an important anisotropy of the OH^- diffusion in lithium niobate crystals. Compared with the results for the z diffusion, the present results show a little larger activation energies, but a very significant increase of the preexponential factors. Differences appear also among the x-cut and y-cut sample results.

Direction of OH^- diffusion	D_{H0} ($cm^2\ s^{-1}$)	E_a (eV)
y-axis	0.07 ± 0.03	1.05 ± 0.05
x-axis	24 ± 15	1.2 ± 0.1
z-axis (Ref. [4])	$(1.4 \pm 0.5)\ 10^{-3}$	0.95 ± 0.02

TABLE 1 Summary of the values for preexponential factors and activation energies of proton diffusion in different crystallographic directions of $LiNbO_3$:Fe crystals, obtained from photorefractive fixed hologram decays

It is interesting to note that the degree of anisotropy obtained in this work for lithium niobate is similar to that measured in TiO_2 [9]: a little higher activation energy but several orders of magnitude higher preexponential factor for the direction perpendicular to the z-axis as compared with that parallel to it. Similarly, the OH stretching absorption band is also absolutely σ-polarized in rutile. Then we can interpret the anysotropy as a result of a different diffusion mechanism along each direction. Let us think on the proton diffusion in the lithium niobate lattice. Assuming that the O—H bond is pointed to a nearest oxygen atom in the atomic plane perpendicular to the z-axis, we could expect a high number of jumping attempts per second to move to the nearest oxygen ion. This leads to a high preexponential factor. In contrast, the diffusion along the z-axis needs to follow a zigzag path from a plane of oxygens to the next one. This movement is in a different direction of the stretching vibration mode of the O—H bond. It seems reasonable to expect a very much lower number of jumping attempts per unit time in this case.

Similarly, one could explain the difference in activation energy in the following way: For diffusion in the oxygen plane the proton has to jump from one oxygen ion to the next one. To continue the diffusion in the same direction, this jump has to be followed by a bond rotation of 180° around the new oxygen ion in the plane. Similar rotation has been invoked for proton diffusion in TiO_2 [18]. Then two processes are involved. In contrast, for diffusion in the z-direction the bond needs a smaller rotation. Thus, one could understand a little lower activation energy for this second process, as it is observed.

4 Conclusions

In summary, we were able to storee and fix, for the first time, holograms with K-vector oriented in perpendicular to the z-axis of lithium niobate crystals. Notwithstanding, the

diffraction efficiency showed by these holograms is quite reduced compared with that of usual holograms in this material. Measurements of diffraction efficiency time decays for these new holograms at different temperatures allowed us to determine the diffusion coefficient of protons, and its thermal dependence, along directions perpendicular to the z-axis $LiNbO_3$. A significant anisotropy has been found in both the preexponential factor and the activation energy. It is worthwhile to note that this method involving photorefractive measurements allow determining the bulk diffusion constant, avoiding the possible distortions that could be introduced by dislocations or other defects present in the crystal.

ACKNOWLEDGEMENTS This work was partially supported by the Spanish Ministerio de Ciencia y Tecnología under Grant No. TIC2001-0605.

REFERENCES

1 J.J. Amodei, D.L. Staebler, Appl. Phys. Lett. **18**, 540 (1971)
2 H. Vormann, G. Weber, S. Kapphan, E. Krätzig, Solid State Commun. **40**, 543 (1981)
3 K. Buse, S. Breer, K. Peithmann, M. Gao, E. Krätzig, Phys. Rev. B **56**, 1225 (1997)
4 E.M. de Miguel-Sanz, M. Carrascosa, L. Arizmendi, Phys. Rev. B **65**, 165101 (2002)
5 W. Meyer, P. Würfel, R. Munser, G. Müller-Vogt, Phys. Status Solidi A **53**, 171 (1979)
6 C.R. Hsieh, S.H. Lin, K.Y. Hsu, T.C. Hsieh, A. Chiou, J. Hong, Appl. Opt. **38**, 6141 (1999)
7 L. Arizmendi, E.M. de Miguel-Sanz, M. Carrascosa, Opt. Lett. **23**, 960 (1998)
8 J.R. Herrington, B. Dischler, A. Räuber, J. Schneider, Solid State Commun. **12**, 351 (1973)
9 O.W. Johnson, S.H. Paek, J.W. DeFord, J. Appl. Phys. **46**, 1026 (1975)
10 H. Engstrom, J.B. Bates, J.C. Wang, M.M. Abraham, Phys. Rev. B **21**, 1520 (1980)
11 L. Kovacs, M. Wohlecke, A. Jovanovic, K. Polgar, S. Kapphan, J. Phys. Chem. Solids **52**, 797 (1991)
12 R. Gonzalez, Y. Chen, K.L. Tsang, G.P. Summers, Appl. Phys. Lett. **41**, 739 (1982)
13 H. Kurz, E. Krätzig, W. Keune, H. Engelmann, U. Gonser, B. Dischler, A. Rauber, Appl. Phys. **12**, 355 (1977)
14 E.M. de Miguel, J. Limeres, M. Carrascosa, L. Arizmendi, J. Opt. Soc. Am. B **17**, 1140 (2000)
15 J.D. Zook, D. Chen, G.N. Otto, Appl. Phys. Lett. **11**, 159 (1967)
16 H.G. Festl, P. Hertel, E. Krätzig, R. von Baltz, Phys. Status Solid B **113**, 157 (1982)
17 B.I. Sturman, V.M. Fridkin, *The Photovoltaic and Photorefractive Effects in Noncentrosymmetric Materials* (Gordon and Breach, Amsterdam, 1992), p. 13
18 J.B. Bates, J.C. Wang, R.A. Perkins, Phys. Rev. B **19**, 4130 (1979)